

# Effects of Nested Area Size upon Regional Climate Model Simulations<sup>①</sup>

Liu Huaqiang (刘华强)

P4 A

*Laboratory for Meteorological Disasters and Environmental Change, Nanjing Institute of Meteorology, Nanjing 210044*

Qian Yongfu (钱永甫)

*Department of Atmospheric Sciences, Nanjing University, Nanjing 210093*

Zheng Yiqun (郑益群)

*Nanjing Institute of Geography and Limnology, Chinese Academy of Sciences, Nanjing 210008*

(Received January 22, 2001; revised September 25, 2001)

## ABSTRACT

This paper presents a numerical study on the 1998 summer rainfall over the Yangtze River valley in central and eastern China, addressing effect of a nested area size on simulations in terms of the technique of nesting a regional climate model (RCM) upon a general circulation model (GCM). Evidence suggests that the size exerts greater impacts upon regional climate of the country, revealing that a larger nested size is superior to a small one for simulation in mitigating errors of GCM-provided lateral boundary forcing. Also, simulations show that the RCM should incorporate regions of climate systems of great importance into study and a low-resolution GCM yields more pronounced errors as a rule when used in the research of the Tibetan Plateau, and, in contrast, our P $\sigma$ RCM can do a good job in describing the plateau's role in a more realistic and accurate way. It is for this reason that the tableland should be included in the nested area when the RCM is employed to investigate the regional climate. Our P $\sigma$ RCM nesting upon a GCM reaches more realistic results compared to a single GCM used.

**Key words:** Regional climate model, Atmospheric general circulation model, Nesting

## 1. Introduction

Numerous significant findings have been achieved from the studies of large-scale climate variation by atmospheric general circulation models (Gates, 1992) but these models do not work well in the research of modeling and prediction of regional climate variation (Groth and MacCracken, 1991). For more details of regional climate, one of the approaches has in the past decade been the use of nesting RCMs on GCMs, most popular being "one-way nesting" at present, and in China the study of high-resolution RCM simulation has been undertaken mainly in the latest few years (Zhao and Luo, 1998) and almost all researchers adopted RCMs rather than use GCMs with increased horizontal resolution or variable-grid global models.

RCM boundary values for forcing taken from observations are regarded as "precise". It is found that with equal boundary buffer zone's width available, the smaller the model

<sup>①</sup>This work was supported by the National Natural Science Foundation of China under Grant No 49735170.

domain, the closer the simulation to the measured field. Thus, we are led to believe that in an extreme case a simulated value equals a measured one if a model domain becomes a "point". But the ultimate goal of regional climate research is to predict its variation and thus, the RCM has to be nested upon the GCM—given boundary values that are, however, inevitably in errors, during which the RCM nested area size exerts influence on simulations that may differ somewhat from what is mentioned just above. In previous RCM studies it was a common practice to extend outward more or less arbitrarily a target zone in delineating a model domain, neglecting the significance of a model zone scale to output. With this consideration in mind, we conducted experiments to explore effects of a nested area size upon simulation when a RCM is nested upon a GCM.

## 2. Brief model description and experimental scheme

The prototype GCM was proposed by Bourke et al. (1977) and McAvaney et al. (1978) and developed by Simmonds (1985) and Lin (1991) into an AGCM that contains 9 levels in vertical and truncated rhomboidally at wavenumber 15 (referred to as an L9R15 model hereafter). The L9R15 adopts  $\sigma$  coordinate vertically and Monin–Obukhov parameterization for the boundary layer, including in itself the effects of surface roughness, moisture, sea surface temperature, polar ice cover and those of clouds, vapor, CO<sub>2</sub> and O<sub>3</sub> on radiation. This work employed the prototype L9R15 containing daily variation in solar radiation (Shao et al., 1998).

The regional climate model in a P– $\sigma$  coordinate system (P $\sigma$ RCM) for this study is constructed on the basis of a primitive equation model produced by Qian (1985), with physics and vertical structure almost identical to those of the original model except increased horizontal resolution of  $1^\circ \times 1^\circ$ , the specific humidity field calculated at each time step instead of every hour, a parameterization scheme based upon the Monin–Obukhov similarity theory utilized for PBL momentum, heat and vapor fluxes (Zhang and Qian, 1999), but with the soil and ocean submodels of the original model preserved. The integration scheme consists of 1 h Euler's backward difference alternate with 5 h central difference operated at 3 min timestep. It is found that the P $\sigma$ RCM using observations as a forcing has a quite high capability to imitate the variation of regional climate in China (Liu and Qian, 1999).

The P $\sigma$ RCM has as its lateral boundary the sponge limit with one-way nesting tendency correction and its lateral boundary buffer zones take 8 model boundary cycles whose weighed coefficients  $w(n)$  vary exponentially in the normal direction. And the boundary conditions are given by

$$\left(\frac{\partial \alpha}{\partial t}\right)_n = (1 - w(n))\left(\frac{\partial \alpha}{\partial t}\right)_{MC} + w(n)\left(\frac{\partial \alpha}{\partial t}\right)_{LS}, \quad (1)$$

$$w(n) = \exp\left(-\frac{n-1}{3}\right), \quad (n = 1, 2, \dots, 8) \quad (2)$$

where  $n$  stands for the serial number of a gridpoint inward along the normal,  $\alpha$  for a variable, subscript MC for tendency obtained from the P $\sigma$ RCM and subscript LS for large-scale tendency forcing given by GCM or measurements.

The exceptional great flood event in 1998 over the middle and lower reaches of the Yangtze River was taken for a case study. One P $\sigma$ RCM study was undertaken using NCEP reanalyses as a forcing to examine the model ability to imitate regional climate, then the L9R15 imitation was performed in order to compare with the results from its nesting with our

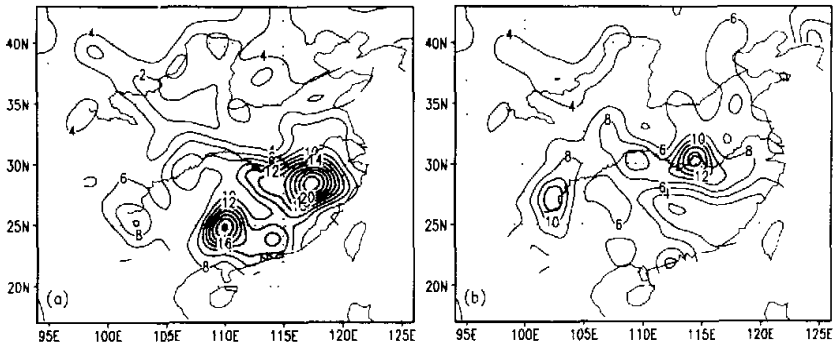


Fig. 1. Precipitation rates (mm / day) measured in June (a) and July (b) in 1998.

P $\sigma$ RCM in which effect of a nested area size was investigated on simulations.

For all the above experiments, integration was begun from 0000 GMT, 1 May 1998 for which the initial fields were based on daily NCEP reanalyses and the SST field on 1998 weekly means at  $1^{\circ} \times 1^{\circ}$  resolution on a global basis to which linear interpolation was performed to get daily mean SST data that were offered to the L9R15 or P $\sigma$ RCM. Besides, the L9R15 employed climatological snow and ice cap.

### 3. Verification of P $\sigma$ RCM simulations

Figure 1 portrays the field of measured precipitation in June and July, 1998, indicating that in June rainfall occurred mainly south of the middle and lower reaches of the Yangtze River and in parts of South China (stippled) and was of high intensity and extensive, reaching monthly total of 500–700 mm locally, and in July the rain belt (RB) was chiefly located in the middle reaches with less strength than in June. The RB is markedly southward of climatological mean for the same period, thereby prolonging the rainfall season so as to produce a great flood event in the research basins.

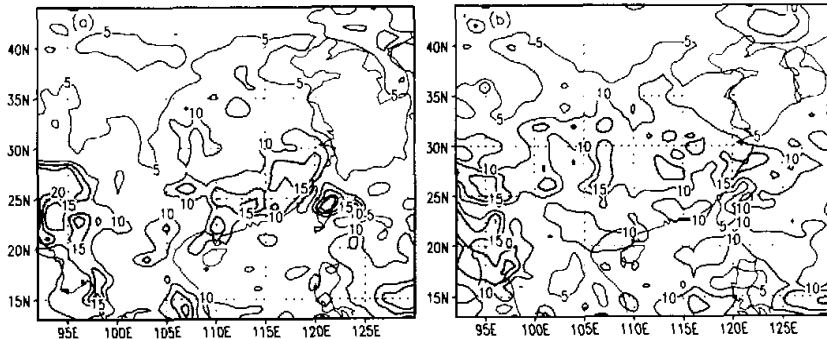


Fig. 2. As in Fig. 1 but based on P $\sigma$ RCM simulations.

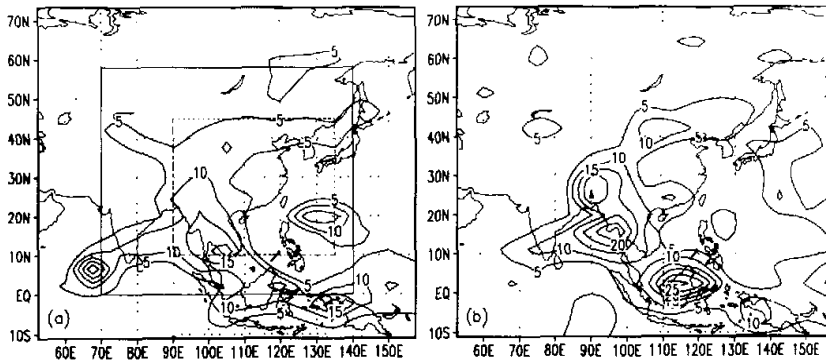


Fig. 3. The same as in Fig.1 but from L9R15 imitations.

The domain of P $\sigma$ RCM simulations using daily NCEP data as boundary forcing is presented in the inner dashed box of Fig. 3a. The distributed rainfall rates from the P $\sigma$ RCM simulations for June and July are drawn in Figs. 2a and 2b, respectively. Inspection of Figs. 2 and 1 shows that the P $\sigma$ RCM has capability to imitate dominant RBs, on the whole, inside China for the two months, indicating the viability of the model. Also, we notice therefrom that because of the adopted lateral boundary forcing given by observations, the resulting simulations compare more favorably with the P $\sigma$ RCM–L9R15 nesting that will be given in a later section. This illustrates that a precise lateral boundary forcing is absolutely necessary for the regional climate simulation.

#### 4. L9R15 simulations

Figures 3a, b illustrate L9R15–simulated distribution of Asian rainfall rates (mm./day) for June and July, 1998, indicating that the RBs are situated largely on the north and south sides of the western Pacific subtropical high, the northern one responsible for the 1998 calamity in the study valleys and we now focus on this RB. Examination discovers greater difference in position between the imitated and observed. The dominant RB duplicated for the two months is in North China with the locality remarkably northward compared to the observed although a secondary one is reproduced in July in the southern part except for unsimulated rainfall over the valleys, thus indicating that as a low–resolution global model the L9R15 has lower ability to imitate regional precipitation.

As evidenced from the foregoing study, the L9R15 rainbelt is positioned significantly northward, making feel the need of examining the L9R15–simulated pressure system, with the monthly mean height delineated separately in Fig. 4 for June and July in contrast to the corresponding fields after NCEP reanalyses in Fig. 5. Their comparison shows the difference between the duplicated and observed pattern largely in the following: 1) the simulated ridge in East China and its seaboard are considerably enhanced, exhibiting itself as a spurious feature this overestimated ridge gets intensified steadily from June to July and superimposed in July upon the subtropical high, thereby making the latter have the vigor above normal; 2) the imitated 500 hPa height over the Tibetan Plateau is much lower compared to the observed field, displaying itself as a false trough, which gets steadily deepened in this period. Evidently,

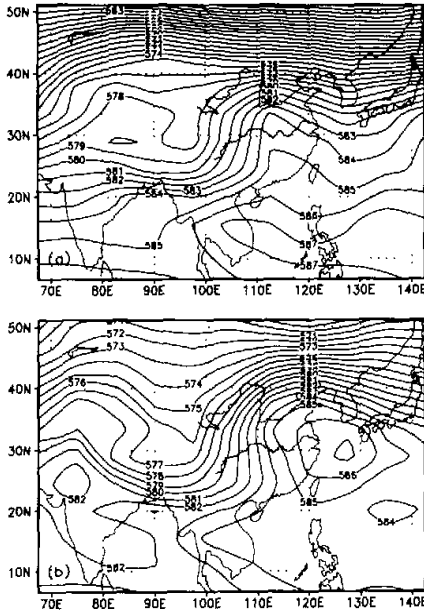


Fig. 4. L9R15-given 500 hPa geopotential height (dam) for June (a) and July (b).

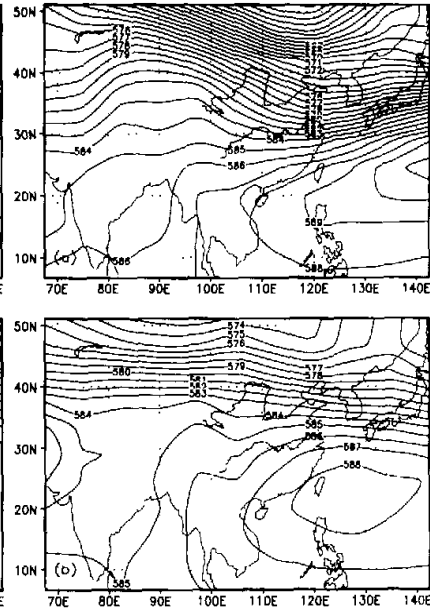


Fig. 5. As in Fig. 4 except for the NCEP reanalysis-drawn height field.

existence of the spurious ridge to the east of the Plateau serves as the dominant cause of the northward displacement of the simulated RB. And error of the 500 hPa height imitation is available in the two months, indicative of the systematic error inherent in the model.

The genesis of the false ridge bears an intimate relation to the development of the spurious low over the Tibetan Plateau to the west. When a thermal low develops vigorously over the Plateau in summer, so does the subtropical high downstream, a relationship that has been substantiated by numerous studies, the dominant role played by thermal effect of the tableland. The L9R15 is defective in easily generating a "false" pressure system over large-scale terrestrial giants, e.g., the Tibetan Plateau, Rockies, Andes and the Antarctic because of its low resolution (Wu et al., 1996). We can thus assume that the northward position of the duplicated RB is due mainly to the L9R15 low-resolution errors for the plateau which is unable to accurately describe thermal and dynamic effects produced by the extensive tableland.

## 5. Experiments with our P $\sigma$ RCM nested upon L9R15

Two experiments were developed, one being a larger-area nesting (denoted by DMB) and the other being a small one (DML). The former has its nested area of 0°–58°N, 70°–140°E with gridpoint total of 71 × 59 with the inclusion of the Tibetan Plateau, as shown in the outer box (solid line) of Fig. 3a and the latter (DML) covers 10°–45°N, 90°–135°E.

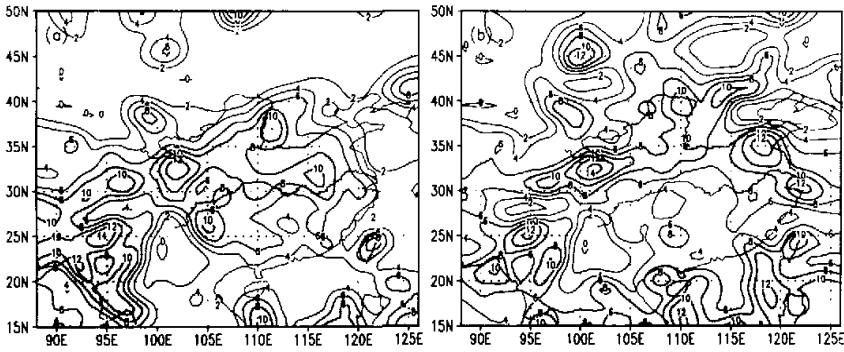


Fig. 6. DMB-given rainfall rates (mm / day) for June (a) and July (b)

totaling in gridpoints of  $46 \times 36$ , including part of the Plateau, as is shown in the inner box (dashed line enclosed) of the same figure. For the P $\sigma$ RCM, the lateral boundary forcing is renewed at 12 h intervals with the aid of related instantaneous output field from the L9R15.

### 5.1 DMB run-given simulations

Figure 6 presents the patterns of DMB-exported precipitation in June and July, 1998. Comparison of Figs. 6 and 3 shows that the imitated RB, despite being more or less northward, is moved considerably southward compared to L9R15 outcome and somewhat intensified. Consequently, the DMB results are closer to the observed with simulations greatly better compared to the L9R15 findings. It follows that simulations are a lot better from DMB than from L9R15 experiment for the 1998 wet-period rainfall, which mitigates the unduly northward position of the L9R15 rainband to some degree, thus demonstrating preliminarily that the GCM-RCM nesting yields better results than the single GCM is employed for short-term climate research.

It should be noted that the RB from the P $\sigma$ RCM nested on L9R15 remains more northward than the observed, which is far poorer than when NCEP reanalysis is used as lateral boundary forcing, a fact which is related to inappropriate forcing by L9R15. Moreover, L9R15-given RB is unduly northward with the consequence that, although P $\sigma$ RCM can capture more effectively GCM-unidentifiable forcing of region-scale topography and surface features upon regional climate variation, it is unable to improve simulations to great extent simply due to errors that GCM offered lateral boundary forcing, which lead to the L9R15 rainband moved unduly northward.

Figure 7 presents DMB-given monthly mean 500 hPa height over June and July. As stated before, the geopotential height patterns differ more greatly between the L9R15 outcome and NCEP reanalyses. Comparison of Figs. 7 and 4 indicates that the DMB run did not produce a false trough over the study plateau nor a spurious ridge in East China, leading to the DMB-produced RB southward of the L9R15 analog. Further, comparison of Figs. 5 and 7 reveals that the DMB imitated geopotential height field is closer to the NCEP pattern, i.e., a weak ridge over the plateau and to its north, a phenomenon that is related to the anticyclonic curving of westerly flow around the plateau; both the fields display a southerly branch trough on the south side, portraying a clear feature with a ridge (trough) on the north (south) side and sparsely-distributed contours above the plateau. Moreover, Figs. 7a, b show a semi-cast

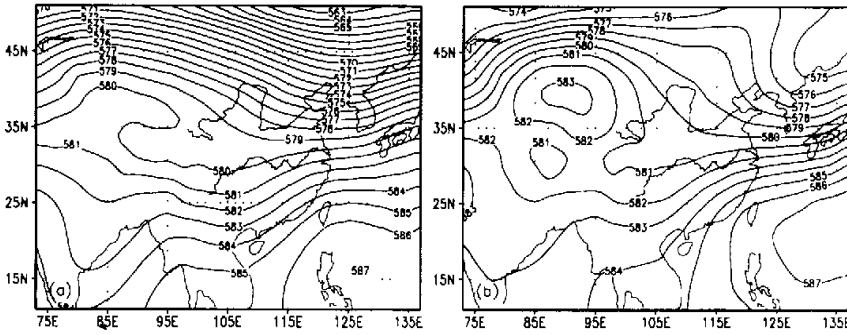


Fig. 7. DMB-given monthly mean 500 hPa height (dam) for June (a) and July (b).

to west shear simulated in  $30^{\circ}$ – $35^{\circ}$ N, with a high's center to the north, a situation favorable for precipitation occurrence in the middle and lower reaches of the Yangtze River.

From the foregoing analysis we notice that the nesting  $P\sigma$ RCM upon L9R15 will better considerably the simulation of 500 hPa height, especially in the research plateau, which is attributed to higher horizontal resolution of the  $P\sigma$ RCM for identifying more realistic regional topography and a higher-precision pressure gradient force calculating scheme whereby it is likely to describe effect of the plateau upon atmospheric motion in a more detailed and accurate manner, thus effectively making up the deficiency of the L9R15 in simulating the plateau's role.

### 5.2 DML given simulation

Figures 8a, b are the distribution of DML precipitation rates (mm/day) in June and July, respectively, displaying that the June imitated RBs are located dominantly north of the Yangtze River and composed of two rainbands, one being the northern one around  $40^{\circ}$ N and the southern one about  $34^{\circ}$ N, a situation that illustrates a quite large difference from the in situ observations despite some southward displacement versus the L9R15 simulation. And for July the DML rainbands are still more northward (largely north of the Yellow River) as against the observed analogs but close to the L9R15 outcome. In comparison to the DMB simulation, the DML output is considerably poorer, leading to simulated rainfall located far northward, close to the L9R15 rainbands, indicating that in the small nested area the RCM lowers the improvement on the L9R15 results, making them even closer to those when the L9R15 offers a large-scale background field for simulation.

From the comparison of Figs. 9a, b (for DML monthly mean height) to Figs. 7a, b (for DMB counterpart), we see that the DML nested box is small enough to exclude the plateau as a whole with the result that we can investigate only the geopotential height to the east. Inspection reveals that the DML false ridge in the eastern seaboard remains and strengthens steadily from June to July, a result that is in concord with the L9R15 equivalent. It follows that the DML does not effectively get rid of the appearance of the spurious ridge given by L9R15, a fact that is in agreement with the more northward RBs from the DML compared to the DMB outcome. It can be inferred thereby that the DML box did not cover the entire plateau and so not better greatly the situation for weakening the false ridge.

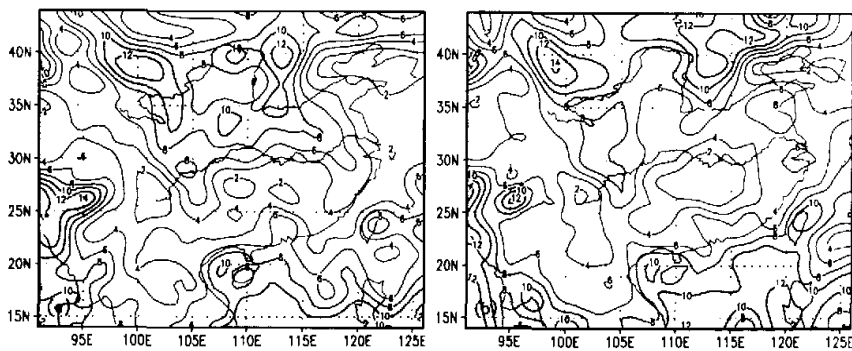


Fig. 8. The same as in Fig. 6 but for DML outcome.

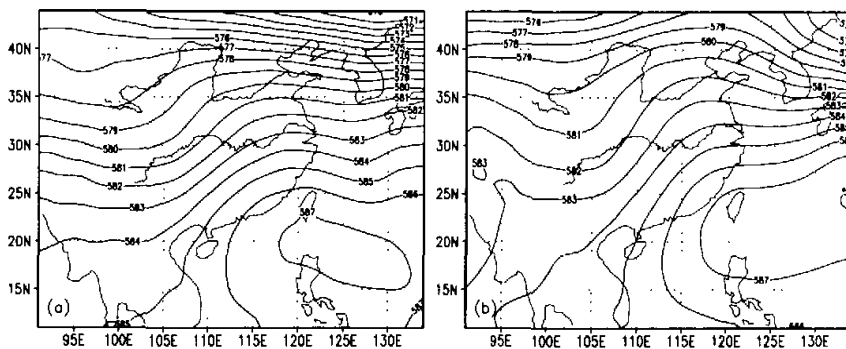


Fig. 9. DML-given monthly mean 500 hPa height (dam) for June (a) and July (b).

## 6. Discussion and conclusions

The above experiments show that when the GCM-RCM nesting technique is used in the study of regional climate in China, the nested area size has rather great effect on simulations due to the fact that GCM-furnished boundary forcing has certain error and it is found that a larger size yields better result. This is related to the fact that 1) the RCM requires sufficient space and time to develop region-scale climate systems based upon forcing inside the box in order to mitigate effect of large-scale background errors in boundary's buffer-zone so that if the nested zone were too small, then the contribution of RCM internal forcing would be so, leaving output under greater control of GCM-given large-scale background, resulting in insignificant improvement on GCM simulation, which agrees well with Giorgi et al. (1993), and 2) nesting RCM upon GCM has as its aim to better description of forcing on regional climate variation in related surface features, thus leading to the fact that we should try to include a nested-area innegligible factors (e.g., plateau and mountains) affecting regional climate, particularly areas with pronounced climate regionality. Improvement of GCM fore-



casts is undoubtedly critical to the nesting climate simulation.

It should be noted that this article presents only qualitative conclusions from the study of the 1998 flood event over the middle and lower reaches of the Yangtze River drainage area. However, for different factors or events and their geographic positions, the RCM domains should differ to some extent. As a result, quantitative conclusions should be based on simulations of dissimilar cases in terms of different models.

From this study, we come to the dominant conclusions as follows:

(1) The RCM nested on GCM can ameliorate the simulation of climate in China but different-size RCM domains reveals dissimilar effects on outcome. When GCM-produced boundary forcing possesses certain errors, a larger nested section should be taken for better output, and v.v. for this reason it is inappropriate to take a smaller-size RCM box for numerical study.

(2) In accordance with a research factor and its position, the RCM-covered area should incorporate in itself regions of important climate systems. As stated earlier, the Tibetan Plateau has innegligible impacts on the climate of China and the low-resolution GCM gives greater errors for the plateau. And the RCM is able to describe the plateau's thermal and dynamic effects in a more realistic and accurate way than a GCM such that a nested box should include in itself the Plateau to make up the deficiency in GCM simulation of the plateau, thus rendering the RCM nesting upon a GCM better than a single GCM used as regards the simulations, at least in the imitation of summer precipitation over the Yangtze River valley.

## REFERENCES

- Bourke, W., B. McAvaney, K. Puri, and R. Thurling, 1977: Global modeling of atmospheric flow by spectral methods. *Method in Computational Physics*, Academic Press, 267-324.
- Gates, W. L., 1992: The atmospheric model intercomparison project. *Bull. Amer. Meteor. Soc.*, **73**, 1962-1970.
- Giorgi, F., M. R. Marinucci, G. T. Bates, and G. De Canio, 1993: Development of a second-generation regional climate model (RegCM2). Part II: Convective processes and assimilation of lateral boundary condition. *Mon Wea. Rev.*, **121**, 2814-2832.
- Groth, S. L., and M. C. MacCracken, 1991: The use of general circulation models to predict regional climate change. *J. Climate*, **4**, 286-303.
- Lin Yuanbi, 1991: General Circulation Experiments at Guangzhou Institute of Tropical Oceanography and Meteorology, 14pp.
- Liu Huaqiang, and Qian Yongfu, 1999: Numerical simulations of intensive Meiyu rainfall in 1991 over the Changjiang and Huathe River valleys by a regional climate model with  $P-\sigma$  incorporated coordinate system. *Advances in Atmospheric Sciences*, **16(3)**, 395-404.
- McAvaney, B., W. Bourke, and K. Puri, 1978: A global spectral model for simulation of the general circulation. *J. Atmos. Sci.*, **35**, 1557-1583.
- Qian Yongfu, 1985: A five-layer primitive equation model with topography. *Plateau Meteor.*, **4(2)**, 1-28 (sup. issue) (in Chinese).
- Shao Hui, Qian Yongfu, and Wang Qianqian, 1998: The effects of the diurnal variation of solar radiation on climate modeling of L9R15. *Plateau Meteor.*, **17(2)**, 158-169 (in Chinese).
- Simmonds, I., 1985: Analysis of the "Spinup" of a general circulation model. *J. Geophys. Res.*, **90**, 5637-5660.
- Wu Guoxiong, Liu Hui, and Zhao Yucheng, 1996: A nine-layer atmospheric general circulation model and its performance. *Advances in Atmospheric Sciences*, **15(1)**, 1-18.
- Zhang Qiong, and Qian Yongfu, 1999: Effects of boundary layer parameterization on the monthly mean simulation. *Acta Meteorologica Sinica*, **1**, 73-85.
- Zhao Zongci, and Luo Yong, 1998: Advances in regional climate simulation in the 1990s. *Acta Meteorologica Sinica*, **56**, 225-246 (in Chinese).

## 嵌套域大小对区域气候模式模拟效果的影响

刘华强 钱永甫 郑益群

### 摘 要

利用与大气环流模式(GCM)嵌套的区域气候模式(RCM)对1998年中国长江流域夏季降水进行了模拟试验,讨论了嵌套区域大小对模拟效果的影响。结果表明,嵌套域的大小对模拟结果存在较大的影响,由于GCM为区域模式提供的侧边界强迫存在一定的误差,大嵌套域在模拟效果上要优于小嵌套域,因此嵌套区域不宜取得过小。模拟结果还表明,区域模式所取范围应该尽量包括具有重要影响的气候系统所在位置在内,由于低分辨率的GCM往往在青藏高原地区存在较大的误差,而RCM能比GCM更真实、准确地描述高原地形的作用,因此嵌套区域应包含整个青藏高原,以使嵌套模式能较GCM更好地模拟中国区域气候。

**关键词:** 区域气候模式, 大气环流模式, 嵌套